Carbohydrate Polymers 103 (2014) 496–501

Contents lists available at ScienceDirect

Carbohydrate Polymers

journal homepage: www.elsevier.com/locate/carbpol

Evaluation of bacterial cellulose/hyaluronan nanocomposite biomaterials

Ying Li[a,b], Shuang Qing[a], Jianhai Zhou[a,b], Guang Yang[a,b,*]

[a] Department of Biomedical Engineering, College of Life Science and Technology, Huazhong University of Science and Technology, Wuhan 430074, PR China
[b] National Engineering Research Center for Nano-Medicine, Huazhong University of Science and Technology, Wuhan 430074, PR China

ARTICLE INFO

Article history:
Received 21 July 2013
Received in revised form
22 November 2013
Accepted 17 December 2013
Available online 4 January 2014

Keywords:
Bacterial cellulose
Hyaluronan
Nanocomposites
Wound dressing

ABSTRACT

Bacterial cellulose (BC) is useful in the biomedical field because of its unique structure and properties. The high nano-porosity of BC allows other materials to be incorporated and form reinforced composites. Here we describe the preparation and characterization of novel BC/hyaluronan (HA) nanocomposites with a 3-D network structure. BC/HA was obtained using a solution impregnation method. Elemental and ATR-FTIR analyses showed that this method is highly effective to form composites with BC. Weight loss analysis showed that BC/HA have a lower water loss than BC at 37 °C. The total surface area and pore volume of BC/HA films gradually decreased with the HA content, as followed by FE-SEM analysis. The elongation at break of BC/HA films gradually increased as the HA content increased. Thermogravimetric analysis showed that the weight loss for the BC/HA composites were lower than for pure BC between 250 and 350 °C. The results of weight loss, elongation at break and thermal stability suggested that these novel BC/HA films could be applied potentially as wound dressing materials.

1. Introduction

Biological manufacturing has developed rapidly in recent years. Bacterial cellulose (BC) has widespread use in the biomedical field (Czaja, Young, Kawecki, & Brown, 2007), for example as artificial skin, wound dressings (Czaja, Krystynowicz, Bielecki, & Brown, 2006), artificial vessels, scaffolds for tissue engineering (Gao et al., 2011; Svensson et al., 2005), and as meniscal implants (Bodin, Backdahl, Fink, Gustafsson, Risberg, & Gatenholm, 2007). BC is synthesized by *Acetobacter xylinum* and has many unique properties including high biocompatibility, high permeability, good water-holding capacity, mechanical strength, and optimal gelatinization (Klemm, Heublein, Fink, & Bohn, 2005). Purified BC films become transparent after air-drying at room temperature, so when BC is used as a wound dressing or artificial skin, the wound healing can be monitored.

Many efforts have been devoted to the development of BC-based composites, such as BC/alginate (Chiaoprakobkij, Sanchavanakit, Subbalekha, Pavasant, & Phisalaphong, 2011), BC/silica (Ashori, Sheykhnazari, Tabarsa, Shakeri, & Golalipour, 2012), BC/collagen (Brackmann, Zaborowska, Sundberg, Gatenholm, & Enejder, 2012), BC/chitosan (Ciechanska, 2004), BC/silver nanoparticles (Maneerung, Tokura, & Rujiravanit, 2008) and BC/polyaniline composites (Shi et al., 2012). BC is used as skin tissue repair material because of its superior mechanical properties, excellent biocompatibility, and obvious curative effect during wound healing. Hyaluronan (HA) is a linear high-molecular weight polysaccharide with repeat units of N-acetyl-D-glucosamine and D-glucuronic acid, and is a main component of skin epidermis and dermis; it is non-immunogenic and non-thrombogenic. It is also beneficial for the migration, proliferation, and differentiation of cells during the wound healing process (Gao et al., 2010; Prosdocimi, & Bevilacqua, 2012), with a high capacity for lubrication, water sorption and water retention characteristics which are especially useful for skin repair.

However, HA has poor mechanical properties and suffers from rapid degradation and clearance in vivo, which limits its applications in medicine. A combination of BC with HA would be expected to offer novel features as such high mechanical strength, good water absorption and retention, and to be useful for cell proliferation, migration and differentiation. This nanocomposite could therefore have potential applications in wound dressing or as artificial skin.

In the present study, BC was used as a novel polymeric material to prepare nanocomposites incorporating HA. The composites were obtained by dipping wet BC into HA solutions of different concentrations. The fabrication of the novel films were characterized by elemental analysis, ATR-FTIR spectroscopy, FE-SEM and BET analysis, weight loss analysis, mechanical strength test and thermo gravimetric analysis.

* Corresponding author at: Department of Biomedical Engineering, College of Life Science and Technology, Huazhong University of Science and Technology, Wuhan 430074, PR China. Tel.: +86 278 779 3523; fax: +86 278 779 2265.
E-mail address: yang_sunny@yahoo.com (G. Yang).

0144-8617/$ – see front matter © 2013 Elsevier Ltd. All rights reserved.
http://dx.doi.org/10.1016/j.carbpol.2013.12.059

2. Materials and methods

2.1. Preparation of BC and BC/HA films

BC was biosynthesized by *Gluconacetobacter xylinus* (ATCC53582). The bacteria were grown on a Hestrin and Schramm (HS) medium containing citric acid 0.15% (w/v), disodium phosphate (Na_2HPO_4) 0.27% (w/v), yeast extract powder 0.5% (w/v), peptone 0.5% (w/v), and glucose 2% (w/v) (Hestrin, & Schramm, 1954). The HS medium was sterilized for 20 min at 121 °C. We used the "multilayer fermentation method" and homogenization to obtain the BC films (Fu et al., 2012). The films were dipped into distilled water for 3 days, after incubation for 14 days at 30 °C and a relative humidity level of 30–40%. Bacteria and proteins in the BC films were eliminated by boiling in 1 wt.% NaOH for 30–45 min. Subsequently, the films were washed with distilled water and high-purity water several times until the pH reached 7.0. The films were then sterilized for 20 min at 121 °C and stored in sterilized water at 4 °C.

Hyaluronan (HA; Mw 400–1000 kDa, purity > 98%) was purchased from the Amresco Company. The BC/HA composites were prepared using the solution impregnation method. To ensure complete impregnation of the hyaluronic acid solution in the BC network, the films were dried for 30 min at 37 °C and then dipped into 15 ml of hyaluronan solution (0.05% (BC1), 0.5% (BC2), and 1.0% (BC3) w/v) for about 24 h at room temperature. The BC/HA films were stored at −20 °C for 3 days after draining excess solution, and then at −80 °C for another 2 days. Finally, the BC/HA composites were freeze-dried under vacuum at −50 °C for 2 days (FD-1A-50, China).

2.2. Elemental analysis

The elemental composition of BC, HA and the BC/HA films was determined with a Perkin Elmer analyzer, and using a dynamic combustion method (Vario Micro cube, Elementar Company, Germany). The percentage element composition was obtained.

2.3. Attenuated total reflectance Fourier transform infrared spectroscopy (ATR-FTIR)

The structure of the BC and BC/HA composites with different ratios were investigated by FTIR analysis (VERTEX 70, Bruker, Germany). The spectra were collected over the range from 550 to 4000 cm^{-1} at a resolution of 0.5 cm^{-1}.

2.4. Weight loss analysis

To remove surface water, the wet BC and BC/HA films were quickly shaken twice and then weighed. The wet samples were subsequently dried at 37 °C for 12 h or longer, until their weight became stable, or weighed at different time intervals to monitor the drying process. The percent weight loss of the films was determined using: $w = (w_0 - w_t)/w_0 \times 100\%$, where w_t is the weight of wet films at different time and w_0 is the initial weight, respectively (Nge, Nogi, Yano, & Sugiyama, 2010).

2.5. Field emission scanning electron microscopy (FE-SEM) analysis

The surface morphology and the structure of BC, HA and BC/HA films were characterized by field emission scanning electron microscopy (JSM-6700F, Japan) with an accelerating potential of 5.0 kV and magnifications of 200–10,000. To improve surface conductivity, the freeze-dried samples were sputter-coated with gold for 100 s.

Table 1
Carbon and nitrogen elemental analysis of BC, HA and BC/HA films.

At.%	BC	HA	BC1	BC2	BC3
C	37.28	32.20	41.03	36.61	37.44
N	0.18	2.76	0.33	0.79	1.50

2.6. Brunauer–Emmett–Teller (BET) surface area and pore size analysis

The moisture in the freeze-dried BC and BC/HA composite samples was removed before the BET analysis (BESORP-mini, Japan) by placing them on the sample device and heating up to 120 °C for 6 h, and then cooling to room temperature. The BET surface area and pore size tests used N_2 adsorption at 77 K and an equilibration time of 100 s.

2.7. Mechanical tests

The tensile strength of the wet BC and BC/HA films was measured with a universal testing machine (CMT6503, Shenzhen SANS Test Machine Co. Ltd.). The films were cut into dumbbell-shaped specimens. The distance between the two clamps was 40 mm. All the samples were tested at a stretching speed of 10 mm/min and a humidity level controlled at 60%. The results reported are the average values for $n = 5$ measurements.

2.8. Thermogravimetric analysis (TGA)

TGA measurements for the freeze-dried BC and BC/HA films were done with a thermogravimetric analyzer Model Pyris1 TGA (Perkin Elmer Instruments, China). The degradation of the films was investigated from 25 to 580 °C, under nitrogen atmosphere, at a heating rate of 10 °C/min.

2.9. Statistical analysis

The date are expressed as mean ± standard deviation (SD) and were analyzed statistically by the paired Student's *t*-test method and comparisons among more than two groups were obtained by ANOVA. *p* values less than or equal to 0.05 were considered statistically significant. The statistical significance of differences between groups was performed by using pair-sample *t*-testing method on the Origin 8.0 software.

3. Results and discussion

3.1. Elemental analysis

A dynamic combustion method was used to confirm the composition of the BC/HA nanocomposites. HA consists of repeat units of N-acetyl-glucosamine or glucuronide, but BC has no amide and carboxyl groups. Consequently, thus increasing nitrogen content from 0.33 to 1.50 wt.% in the BC/HA films followed the increasing HA concentration in the impregnation solution. It shows that HA solution successfully infiltrated the BC film network and formed a BC/HA gel composites (Table 1). The nitrogen contents found in the BC and the BC1 samples are not significant since the instrumental error is 0.5%.

3.2. Attenuated total reflectance Fourier transform infrared (ATR-FTIR) spectroscopy

FTIR spectroscopy was used to characterize pure control BC, HA, and modified BC, and the ATR-FTIR spectra were measured from 4000 to 550 cm^{-1}. Fig. 1 shows the absorption peaks for

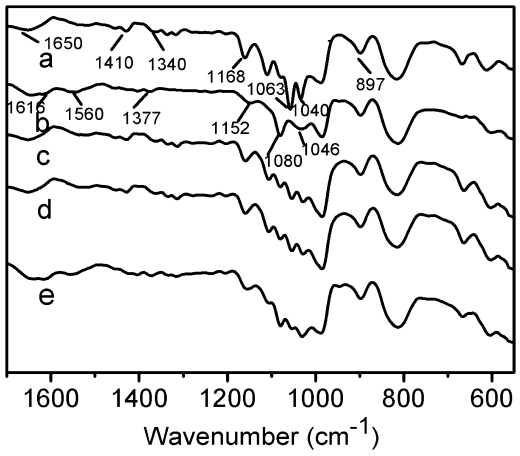

Fig. 1. ATR-FTIR spectra of (a) BC, (b) HA, (c) BC1, (d) BC2 and (e) BC3 from 1650 to 550 cm^{-1}.

BC, HA and the BC/HA composites from 1650 to 550 cm^{-1}. The peaks characteristic for BC in Fig. 1(a) are at 897 cm^{-1} (β-glucosidic linkages between the glucose units), 1040, 1063 cm^{-1} (C—O), 1168 cm^{-1} (C—O—C), 1410 cm^{-1} (—CH_2 or O—H in-plane bending), and 1650 cm^{-1} (H—O—H), respectively (Ashori et al., 2012). The absorption peaks characteristic of HA in Fig. 1(b) are at 1616 cm^{-1} (—COO—), 1560 cm^{-1} (—NH), 1377 cm^{-1} (—CN), 1080 cm^{-1} (C—O), 1152 cm^{-1} (C—O—C), 1046 cm^{-1} (C—OH) and 897 cm^{-1} for the sugar ring anti-symmetric plane vibrations. These results are in good agreement with values previously reported for sodium hyaluronate films (Gilli, Kacurakova, Mathlouthi, Navarini, & Paoletti, 1994). The BC peak is also present in the composites, and the increase in the peaks characteristic for HA at 1616, 1560 and 1377 cm^{-1} can be assigned to the amide I, II, and III bands, respectively. This implies that the HA is bound to the surface of the BC nanofibers, or else incorporated in the amorphous fraction to form the composites.

3.3. Weight loss analysis

The water content and weight loss of films are important when considering their application as wound dressing or artificial skin. In the previous report, Lamke et al. confirmed that the evaporative water loss of different wound degree and granulating wound was from 11.6 ± 1.1 to 214.1 ± 8.4 $g/m^2/h$, while the skin temperature was kept at about 36 °C. The evaporative water loss can be reduced by covering the wounds with dressings. For example, the biological dressings can reduce the water loss by 90%, while the artificial dressings can reduce it by 73% (Lamke, Nilsson, & Reithner, 1977). BC has high water content and displays slow water release or weight loss, which allows it to be widely used as a wound dressing biomaterial (Shezad, Khan, Khan, & Park, 2010; Ul-Islam, Shah, Ha, & Park, 2011). BC is often modified with other materials to decrease its water release properties. HA also has water sorption and retention properties, so the films prepared from these materials were investigated.

The wet samples were weighed at different time intervals to monitor the loss of water at 37 °C at a controlled humidity level of 20%, giving the weight loss as in Fig. 2. The weight loss was fast before 2 h, particularly for BC, and all the samples still displayed significant differences even after 3 h. BC had lost almost all the water after it dried for 3 h. The BC1 and BC2 films were completely dried after 5 h, whereas the BC3 films reached a constant dry weight after 6 h under the same conditions. The weight loss for BC1 was also greater than for BC2 to 3 h, but the opposite trend was observed after 3 h, albeit the differences among these two samples were insignificant. BC1, BC2, and BC3 had lower weight losses than

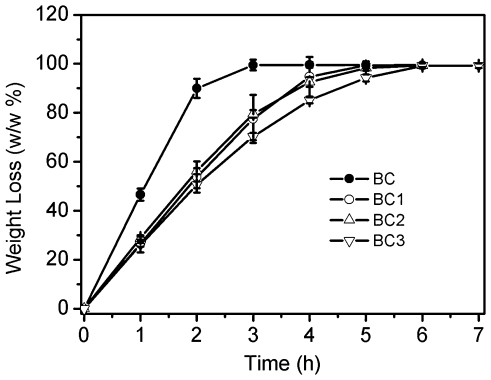

Fig. 2. Water loss from BC and the BC/HA composites as a function of time. Every sample was tested five times and averaged ($n = 5$). The error bars represent the standard deviation on the measurements.

BC, the loss being lowest for BC3. The easier elimination of water from BC films might be due to its larger pore size in comparison to the BC/HA composites. The good water retention characteristics of HA may also have contributed to decreasing the rate of water loss.

Wet environment was needed in wound healing. Lack of water in wound can affect cell metabolism and lead to wound drying. Czaja et al. (2006) studied the applications of BC in the treatment of secondary and tertiary burn. The results showed that BC was a kind of healing-promoted material. The wet environment of BC not only benefits tissue regeneration but also effectively alleviate the pain. The BC/HA composites retained more water than that in BC, and their slower water loss can keep the wound moist for a longer time, which may increase the wound healing capability.

3.4. Morphological characterization of the films

The morphology of the cellulose network and pure HA films were analyzed by FE-SEM; the images obtained are shown in Fig. 3. The HA films appear to have a smooth surface and no obviously pore (B), which might influence the structure of BC. The surface of the BC/HA films is very different from pure BC: The BC/HA samples appear more compact than pure BC. The BC1 film seems to have developed lots of large pores and some lamellar material on it, and as the HA concentration is increased the pore size becomes gradually smaller.

Altmann confirmed that the surface architecture is one of the effective parameters in adhesion and proliferation of the cells and rough surfaces looks more useful for cell adhesion while smooth surfaces better for cell proliferation (Altmann et al., 2013). Sanchavanakit et al. cultured human keratinocytes and fibroblasts on BC. They found that BC films supported the growth, spreading, and migration of human keratinocytes rather than those of human fibroblasts (Sanchavanakit, Sangrungraungroj, Kaomongkolgit, Banaprasert, Pavasant, & Phisalaphong, 2006). FE-SEM results showed that BC/HA composites have a more smooth surface than BC which suggests BC/HA composites may be useful for cell proliferation. HA is useful for cell adhesion, migration, and differentiation, and is involved in a host of cellular processes including morphogenesis, regeneration, and wound healing (Toole, Wight, & Tammi, 2002). Cheng et al. coated HA on RG3/PLGA fibrous scaffolds and HA can completely change the materials from hydrophobicity into hydrophilic, and this hydrophilic materials can promote wound healing in the early stage (Cheng et al., 2013). HA also can sustain various processes such as proteolytic degradation of the provisional matrix to increase cell migration in wound healing (Anilkumar et al., 2011). The FE-SEM results showed that HA successfully bonded with BC in the composite films. The introduction of HA could enhance the hydrophilicity of the composite film

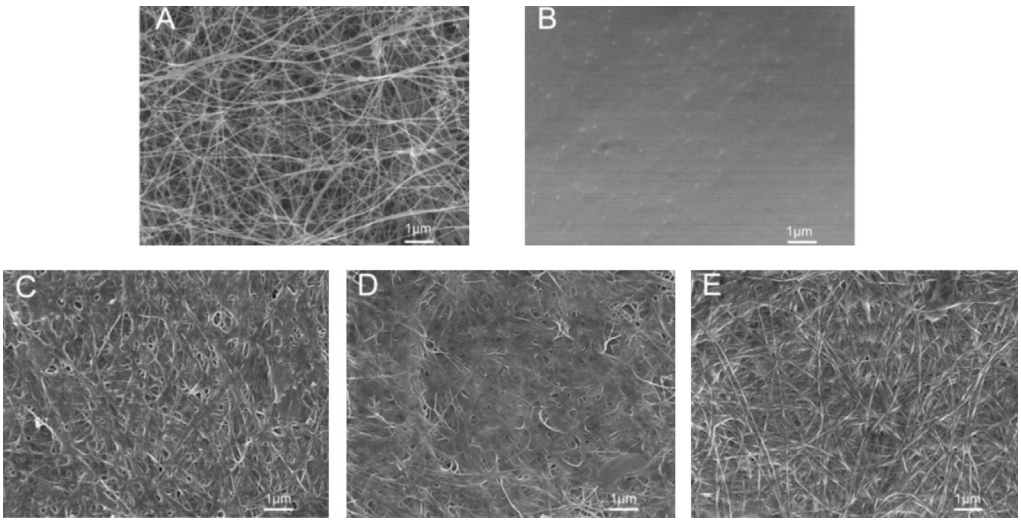

Fig. 3. Surface morphology of BC, HA, and BC/HA composites: (A) BC; (B) HA; (C) BC1; (D) BC2; (E) BC3; the scale bars equal to 1 μm and the magnification is 10,000×.

Table 2
Specific surface area, pore volume and pore diameter analysis for BC and the BC/HA composites prepared at room temperature ($n = 3$).

	Specific surface area (m^2/g)	Specific pore volume (cm^3/g)	Average pore diameter (nm)
BC	60.3 ± 1.1	0.20 ± 0.02	13.29 ± 0.04
BC1	53.4 ± 1.5	0.16 ± 0.01	12.19 ± 0.06
BC2	41.2 ± 1.2	0.14 ± 0.01	12.85 ± 0.03
BC3	39.3 ± 0.1	0.11 ± 0.01	11.15 ± 0.01

surface. BC/HA composites may possess more advantage than pure BC in enhancing the process of wound healing.

3.5. Brunauer–Emmett–Teller (BET) surface area and pore size analysis

The pore size and pore volume of the materials could be quantified from the SEM images, but differences in the porosity are evident in Table 2. Filling of the BC network structure by HA should lead to a reduction of the specific pore volume. The specific surface area, pore size distribution and pore volume of the BC and BC/HA composites were determined by the dead volume measurement method, by applying the BET equation and Barrett–Joyner–Halenda (BJH) method. BJH method was used to analysis of the adsorption branch of the nitrogen isotherm and obtained the pore size distribution curve (Han, Sohn, & Hyeon, 2000). These methods can be used to compare the porous structure of the different samples quantitatively. Fig. 4 and Table 2 both confirm that the HA modification reduced the pore volume and the pore size of the samples.

The specific surface area of the films decreased from 60.3 ± 1.1 to 39.3 ± 0.1 m^2/g from BC to BC3. The specific surface area of the BC/HA films, therefore, gradually decreased with HA content in the composites. Pure BC has the largest surface area. The total pore volume also decreased from 0.20 ± 0.02 to 0.11 ± 0.01 cm^3/g throughout the same sample series. The total pore volume of all the BC/HA films was therefore lower than for BC, BC3 displaying the most obvious difference because of the added amount of HA in the composite.

The pore size distribution curves for all the films are compared in Fig. 4. Even though the pore size distributions for the BC/HA samples appear quite different from BC, the average pore diameter only varied from 13.29 ± 0.04 to 11.15 ± 0.01 nm between BC and various BC/HA composites. This relatively small decrease is nevertheless

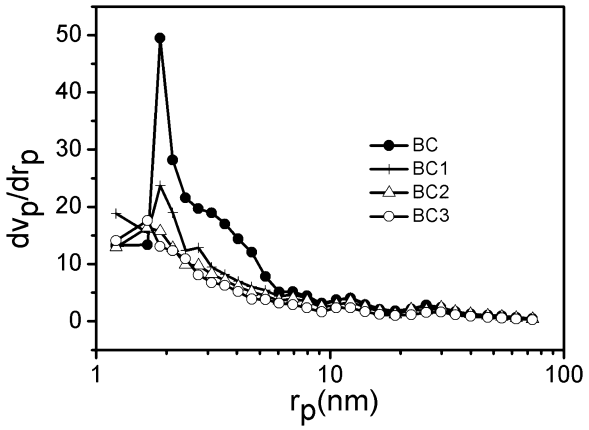

Fig. 4. Pore size distribution in the BC and BC/HA composite films from desorption pore volume BET analysis.

significant because it is larger than the uncertainties of the measurements. This result also matches qualitatively the trends seen in the FE-SEM images in Fig. 3. From the surface area and pore size analysis results, we can conclude that HA influences the structure of BC in the composites.

3.6. Mechanical testing

Properties of good strength, flexibility, bending and sustainability are required by wound dressing materials. Therefore, the tensile strength measurement is often adopted to evaluate the performance of the wound dressing materials (Lee, Park, Hwang, Kim, Kim, & Suh, 2001). The tensile strength (δ) and Young's modulus (E) measured for modified and unmodified BC samples are given in Fig. 5 (right). The tensile strength of BC1 and BC2 was lower than for BC, but the BC3 sample had a higher tensile strength than BC2. This behavior can be attributed to the intermolecular interactions between BC and HA that might reduce the crystallinity and mechanical strength of the composite materials. The Young's modulus of the BC/HA films was lower than for pure BC, showing a decreasing trend with increasing HA concentrations. This effect may be again related to the disruption of intermolecular hydrogen bonding in cellulose, due to the formation of cellulose–hyaluronan hydrogen bonds. As expected, the thickness of the films influenced

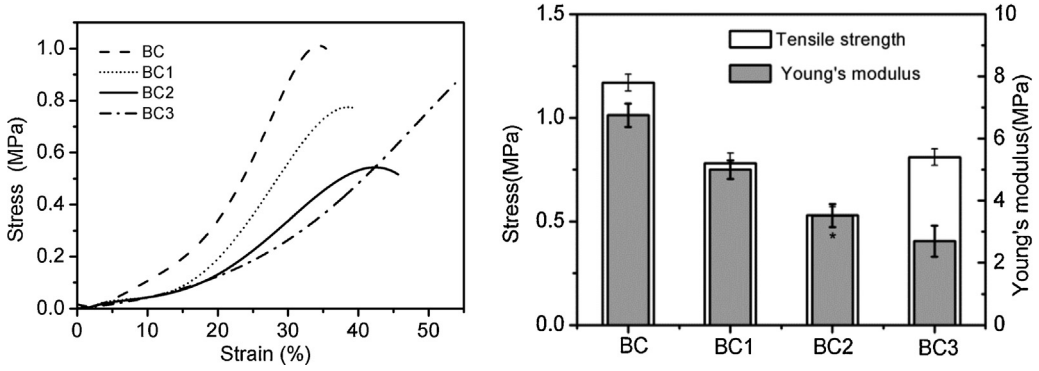

Fig. 5. Strain–stress cures for the BC and BC/HA films (left), tensile strength at breaking point and Young's modulus (right). The data show significant statistical differences between the pure BC (control) and the BC/HA composites ($p < 0.05$, $^{*}p < 0.01$), $n = 5$.

the elongation at break (Fu, Zhou, Zhang, & Yang, 2013). The thickness of BC, BC1, BC2, BC3 was 2.55 ± 0.02, 2.54 ± 0.02, 2.57 ± 0.02 and 2.68 ± 0.03 mm, respectively. While samples BC1, BC2 and BC3 displayed only minor differences in thickness, their elongation at break was significantly different, as shown in Fig. 5 (left). This result correlates well with the amount of HA added. The tensile strength and Young's modulus data show significant statistical differences between the pure BC (control) and the BC1 ($p < 0.05$, $p < 0.05$), BC3 ($p < 0.05$, $p < 0.05$) and BC2 ($p < 0.05$, $p < 0.01$). In comparison with Fig. 5, the elongation at break of the BC/HA films increased whereas the Young's modulus decreased with increasing HA concentrations.

Excellent mechanical strength makes BC attractive as potential wound dressing (Li, Kim, Lee, Kee, & Oh, 2011) and skin repair materials (Czaja et al., 2006, 2007). HA has been shown to play an important role in skin growth by reducing the wound scar (Hu, Sabelman, Cao, Chang, & Hentz, 2003). Wet BC is very soft and its shape can be variable and controllable, which enables BC to contact with the skin completely. Though the tensile strength of composites is lower than that of BC, the elongation at break of BC/HA composites is higher than that of pure BC. We therefore expect that BC/HA should be superior as wound dressing to BC and have the capability to be used as artificial skin.

3.7. Thermogravimetric analysis

The thermal stability of biomedical materials is an important factor influencing their commercial application (Lin & Burggraaf, 1991). The materials must be sterilized at around 121 °C, so they need to be thermally stable. The TGA results for pure BC, HA, and the BC/HA composites are compared in Fig. 6. All the samples display two obvious weight losses. The first weight loss for BC (BC1), HA and the BC/HA (BC2, BC3) films occurred in temperature range from 60 °C to 150 °C, and amount to about 5%, 15%, and 7%, respectively. This could be due to the loss of water by evaporation, or to a reduction in moisture content. The relatively higher weight loss for BC2, BC3 may be due to the water sorption of HA from the environment. BC2 and BC3 composites may absorb more excess exudates than pure BC when they are used as wound dressing. All the samples had a second obvious weight loss starting around 220 °C. This loss is attributed to degradation of the main cellulose skeleton (Li, Jia, Zhu, Ma, & Sun, 2010). The weight loss for the BC/HA composites was lower than for pure BC below 350 °C. These results appear to correlate with the pore size of BC and the HA composites, and the FE-SEM (Fig. 3) and BET analysis (Table 2) results. The BC/HA composites incorporate HA within the BC network structure or on its surface. Moreover, the results might be affected by hydrogen bonding between the BC and HA components of the

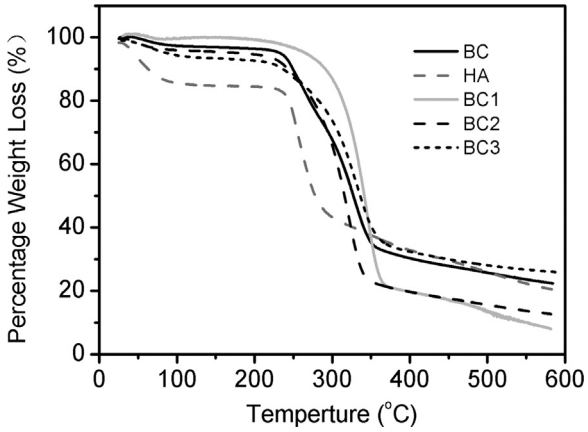

Fig. 6. TGA curves for BC and the BC/HA composites.

composites. This results indicates that BC/HA composites have higher moisture retention ability or lower weight loss than pure BC and HA. BC/HA composites show higher thermal stability than pure BC in the temperature range from 250 to 350 °C.

4. Conclusions

Biocompatible nano-porous films prepared from bacterial cellulose (BC) and hyaluronan (HA) have been produced. Hyaluronan was successfully incorporated into BC using a solution impregnation method. The films contained both BC and HA components, as indicated by FTIR analysis. With increased amounts of HA present the BC/HA films lost water slower than BC under comparable conditions. The elongation at break was higher for BC/HA films than for pure BC, and increased with increasing HA concentrations. The weight loss was lower for the BC/HA composites than for pure BC between 250 and 330 °C. The composites showed enhanced properties in weight loss, elongation at break and thermal stability compared to pure BC, which are important factors for materials applications in biomedical fields. In addition, it has been proved that HA has a positive influence on the healing process (Brenner, Schiffman, Thompson, Toth, & Schauer, 2012). The introduction of HA component could enhance the hydrophilicity of the composite film surface, which would be important for subsequent protein adsorption and consequently the cellular adhesion in the future work. Based on these results, one can conclude that the BC/HA films presented in this work possess superior comprehensive properties, which makes the composite films promising in the application as wound dressing materials such as the skin repair materials.

Acknowledgements

This research was supported by the National Natural Science Foundation of China (21074041), the Fundamental Research Funds for Central Universities, HUST (No. 2010JC016), and the Natural Science of Hubei Province for Distinguished Young Scholars (No. 2008CDB279). The authors are also grateful to Professor Mario Gauthier (University of Waterloo, Canada) for discussion.

References

Altmann, B., Kohal, R., Steinberg, T., Tomakidi, P., Bachle-Haas, M., Wennerberg, A., et al. (2013). Distinct cell functions of osteoblasts on UV-functionalized titanium- and zirconia-based implant materials are modulated by surface topography. *Tissue Engineering Part C: Methods*, *19*(11), 850–863.

Anilkumar, T. V., Muhamed, J., Jose, A., Jyothi, A., Mohanan, P. V., & Krishnan, L. K. (2011). Advantages of hyaluronic acid as a component of fibrin sheet for care of acute wound. *Biologicals*, *39*(2), 81–88.

Ashori, A., Sheykhnazari, S., Tabarsa, T., Shakeri, A., & Golalipour, M. (2012). Bacterial cellulose/silica nanocomposites: Preparation and characterization. *Carbohydrate Polymers*, *90*(1), 413–418.

Bodin, A., Backdahl, H., Fink, H., Gustafsson, L., Risberg, B., & Gatenholm, P. (2007). Influence of cultivation conditions on mechanical and morphological properties of bacterial cellulose tubes. *Biotechnology and Bioengineering*, *97*(2), 425–434.

Brackmann, C., Zaborowska, M., Sundberg, J., Gatenholm, P., & Enejder, A. (2012). In situ imaging of collagen synthesis by osteoprogenitor cells in microporous bacterial cellulose scaffolds. *Tissue Engineering Part C: Methods*, *18*(3), 227–234.

Brenner, E. K., Schiffman, J. D., Thompson, E. A., Toth, L. J., & Schauer, C. L. (2012). Electrospinning of hyaluronic acid nanofibers from aqueous ammonium solutions. *Carbohydrate Polymers*, *87*(1), 926–929.

Cheng, L., Sun, X., Li, B., Hu, C., Yang, H., Zhang, Y., et al. (2013). Electrospun ginsenoside Rg3/poly (lactic-co-glycolic acid) fibers coated with hyaluronic acid for repairing and inhibiting hypertrophic scars. *Journal of Materials Chemistry B*, *1*(35), 4428–4437.

Chiaoprakobkij, N., Sanchavanakit, N., Subbalekha, K., Pavasant, P., & Phisalaphong, M. (2011). Characterization and biocompatibility of bacterial cellulose/alginate composite sponges with human keratinocytes and gingival fibroblasts. *Carbohydrate Polymers*, *85*(3), 548–553.

Ciechanska, D. (2004). Multifunctional bacterial cellulose/chitosan composite materials for medical applications. *Fibres & Textiles in Eastern Europe*, *12*(4), 69–72.

Czaja, W., Krystynowicz, A., Bielecki, S., & Brown, R. M. (2006). Microbial cellulose – the natural power to heal wounds. *Biomaterials*, *27*(2), 145–151.

Czaja, W. K., Young, D. J., Kawecki, M., & Brown, R. M. (2007). The future prospects of microbial cellulose in biomedical applications. *Biomacromolecules*, *8*(1), 1–12.

Fu, L. N., Zhang, Y., Li, C., Wu, Z. H., Zhuo, Q., Huang, X., et al. (2012). Skin tissue repair materials from bacterial cellulose by a multilayer fermentation method. *Journal of Material Chemistry*, *22*(24), 12349–12357.

Fu, L. N., Zhou, P., Zhang, S., & Yang, G. (2013). Evaluation of bacterial nanocellulose-based uniform wound dressing for large area skin transplantation. *Materials Science and Engineering C*, *33*(5), 2995–3000.

Gao, C. A., Wan, Y. Z., Yang, C. X., Dai, K. R., Tang, T. T., Luo, H. L., et al. (2011). Preparation and characterization of bacterial cellulose sponge with hierarchical pore structure as tissue engineering scaffold. *Journal of Porous Materials*, *18*(2), 139–145.

Gao, F., Liu, Y. W., He, Y. Q., Yang, C. X., Wang, Y. Z., Shi, X. X., et al. (2010). Hyaluronan oligosaccharides promote excisional wound healing through enhanced angiogenesis. *Matrix Biology*, *29*(2), 107–116.

Gilli, R., Kacurakova, M., Mathlouthi, M., Navarini, L., & Paoletti, S. (1994). FTIR studies of sodium hyaluronate and its oligomers in the amorphous solid phase and in aqueous solution. *Carbohydrate Research*, *263*(2), 315–326.

Han, S., Sohn, K., & Hyeon, T. (2000). Fabrication of new nanoporous carbons through silica templates and their application to the adsorption of bulky dyes. *Chemistry of Materials*, *12*(11), 3337–3341.

Hestrin, S., & Schramm, M. (1954). Synthesis of cellulose by Acetobacter xylinum. 2. Preparation of freeze-dried cells capable of polymerizing glucose to cellulose. *Biochemical Journal*, *58*(2), 345–352.

Hu, M., Sabelman, E. E., Cao, Y., Chang, J., & Hentz, V. R. (2003). Three-dimensional hyaluronic acid grafts promote healing and reduce scar formation in skin incision wounds. *Journal of Biomedical Materials Research Part B: Applied Biomaterials*, *67*(1), 586–592.

Klemm, D., Heublein, B., Fink, H. P., & Bohn, A. (2005). Cellulose: Fascinating biopolymer and sustainable raw material. *Angewandte Chemie International Edition*, *44*(22), 3358–3393.

Lamke, L., Nilsson, G. E., & Reithner, H. L. (1977). The evaporative water loss from burns and the water-vapour permeability of grafts and artificial membranes used in the treatment of burns. *Burns*, *3*(3), 159–165.

Lee, J. E., Park, J. C., Hwang, Y. S., Kim, J. K., Kim, J. G., & Suh, H. (2001). Characterization of UV-irradiated dense/porous collagen membranes: Morphology, enzymatic degradation, and mechanical properties. *Yonsei Medical Journal*, *42*(2), 172–179.

Li, H. X., Kim, S., Lee, Y., Kee, C. D., & Oh, I. K. (2011). Determination of the stoichiometry and critical oxygen tension in the production culture of bacterial cellulose using saccharified food wastes. *Korean Journal of Chemical Engineering*, *28*(12), 2306–2311.

Li, S., Jia, N., Zhu, J., Ma, M., & Sun, R. (2010). Synthesis of cellulose calcium silicate nanocomposites in ethanol/water mixed solvents and their characterization. *Carbohydrate Polymers*, *80*(1), 270–275.

Lin, Y. S., & Burggraaf, A. J. (1991). Preparation and characterization of high temperature thermally stable alumina composite membrane. *Journal of the American Ceramic Society*, *74*(1), 219–224.

Maneerung, T., Tokura, S., & Rujiravanit, R. (2008). Impregnation of silver nanoparticles into bacterial cellulose for antimicrobial wound dressing. *Carbohydrate Polymers*, *72*(1), 43–51.

Nge, T. T., Nogi, M., Yano, H., & Sugiyama, J. (2010). Microstructure and mechanical properties of bacterial cellulose/chitosan porous scaffold. *Cellulose*, *17*(2), 349–363.

Prosdocimi, M., & Bevilacqua, C. (2012). Exogenous hyaluronic acid and wound healing: An updated vision. *Panminerva Medica*, *54*(2), 129–135.

Sanchavanakit, N., Sangrungraungroj, W., Kaomongkolgit, R., Banaprasert, T., Pavasant, P., & Phisalaphong, M. (2006). Growth of human keratinocytes and fibroblasts on bacterial cellulose film. *Biotechnology Progress*, *22*(4), 1194–1199.

Shezad, O., Khan, S., Khan, T., & Park, J. K. (2010). Physicochemical and mechanical characterization of bacterial cellulose produced with an excellent productivity in static conditions using a simple fed-batch cultivation strategy. *Carbohydrate Polymers*, *82*(1), 173–180.

Shi, Z. J., Zang, S. S., Jiang, F., Huang, L., Lu, D., Ma, Y. G., et al. (2012). In situ nano-assembly of bacterial cellulose–polyaniline composites. *RSC Advances*, *2*(3), 1040–1046.

Svensson, A., Nicklasson, E., Harrah, T., Panilaitis, B., Kaplan, D. L., Brittberg, M., et al. (2005). Bacterial cellulose as a potential scaffold for tissue engineering of cartilage. *Biomaterials*, *26*(4), 419–431.

Toole, B. P., Wight, T. N., & Tammi, M. I. (2002). Hyaluronan–cell interactions in cancer and vascular disease. *The Journal of Biological Chemistry*, *277*(7), 4593–4596.

Ul-Islam, M., Shah, N., Ha, J. H., & Park, J. K. (2011). Effect of chitosan penetration on physico-chemical and mechanical properties of bacterial cellulose. *Korean Journal of Chemical Engineering*, *28*(8), 1736–1743.